

Center
Vortices

Manfried
Faber

Quark
Confinement

Magnetic
Monopoles

Center
Vortices

Structure
Confinement
Area Law

Chiral
Symmetry
Banks-Casher
Dirac Spectrum

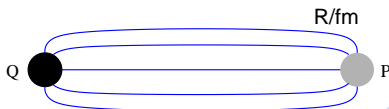
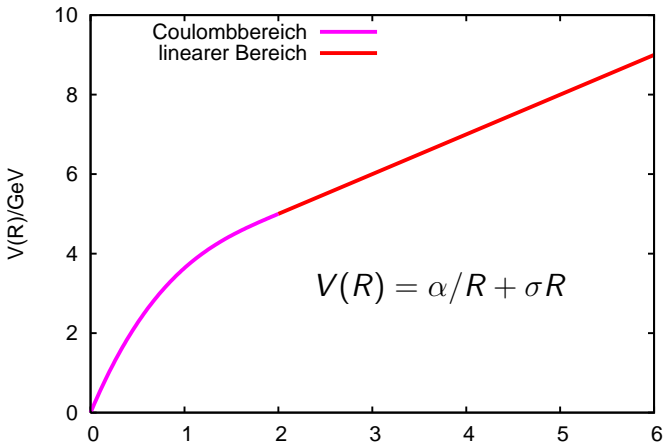
Conclusions



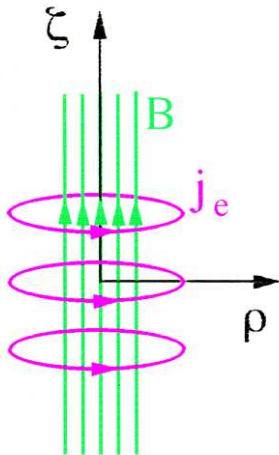
Roman Bertle, Manfried Faber, Roman Höllwieser

Center Vortices, Confinement and Chiral Symmetry Breaking

Michael Engelhardt, Jeff Greensite, Urs Heller,
Gerald Jordan, Stefan Olejnik
Bratislava, New York, San Francisco, Tübingen, Vienna

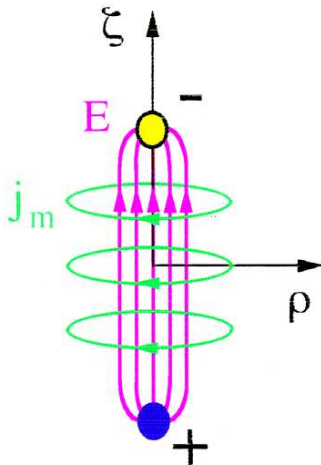


type II superconductor



magnetic fluxoid quantisation

dual superconductor



electric fluxoid quantisation

Center
Vortices

Manfried
Faber

Quark
Confinement

Magnetic
Monopoles

Center
Vortices

Structure
Confinement
Area Law

Chiral
Symmetry
Banks-Casher
Dirac Spectrum

Conclusions

Center Vortices

Manfried Faber

Quark Confinement

Magnetic Monopoles

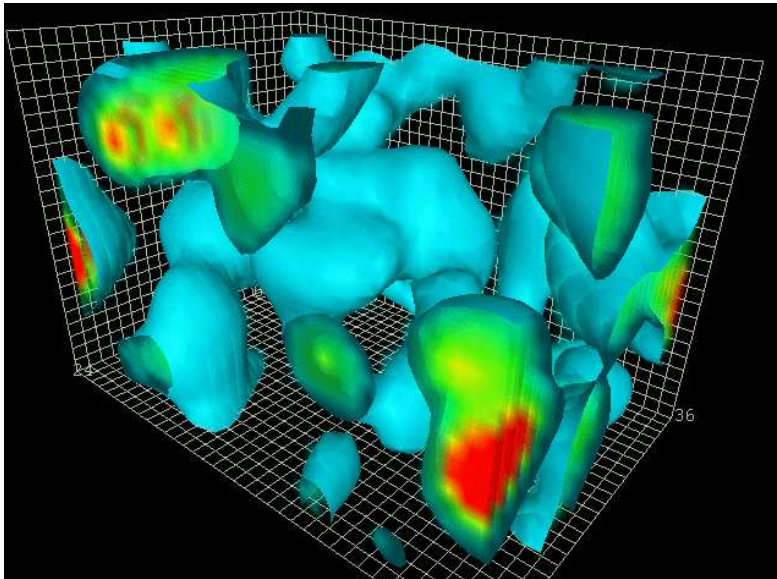
Center Vortices

Structure
Confinement
Area Law

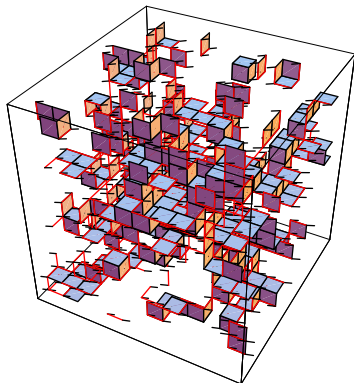
Chiral Symmetry

Banks-Casher
Dirac Spectrum

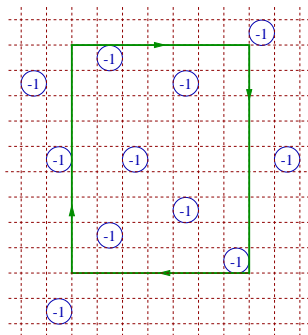
Conclusions



In 4D they form closed 2D-surfaces in Dual Space,
Random Structure



3-dimensional cut through the dual of a 12^4 -lattice.



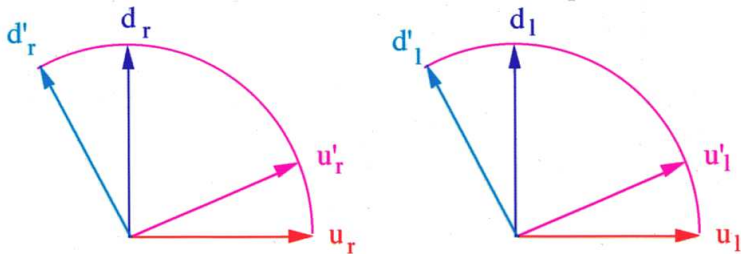
denote f the probability that a plaquette has the value -1

$$\begin{aligned} \langle W(A) \rangle &= [f(-1) + (1-f) \cdot 1]^A = \exp[\underbrace{\ln(1-2f)}_{-\sigma} A], = \\ &= \exp[-\sigma R \times T], \quad \sigma \equiv -\ln(1-2f) \approx 2f \end{aligned}$$

$$m_q + m_{\bar{q}} = 620\text{MeV}, \quad m_{\pi} = 140\text{MeV}$$

⇒ pions near Goldstone bosons of Chiral Symmetry Breaking

QCD dynamics couple quark flavors



Center
Vortices

Manfried
Faber

Quark
Confinement

Magnetic
Monopoles

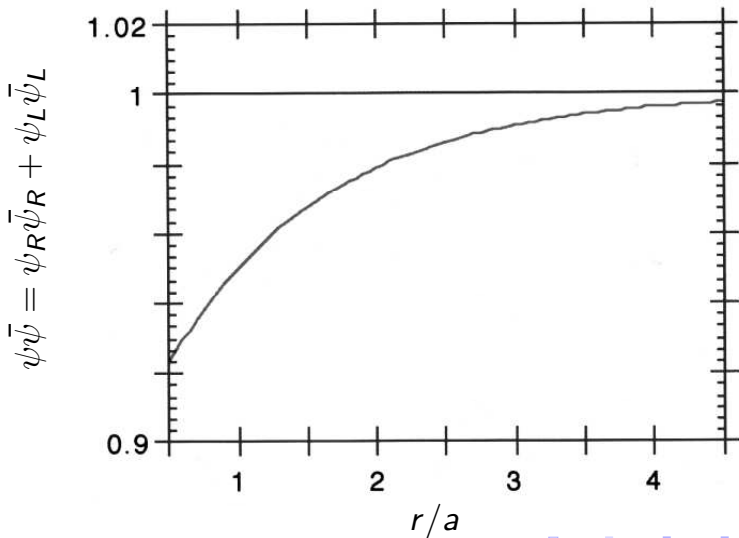
Center
Vortices

Structure
Confinement
Area Law

Chiral
Symmetry

Banks-Casher
Dirac Spectrum

Conclusions



Chiral symmetry breaking \implies
 \implies Low-lying eigenmodes of Dirac operator

$$\bar{\psi}\psi = - \lim_{m \rightarrow 0} \lim_{V \rightarrow \infty} \left\langle \frac{1}{V} \sum_n \frac{1}{i\lambda_n + m} \right\rangle$$

Non-zero eigenvalues appear in pairs $\pm i\lambda_n$

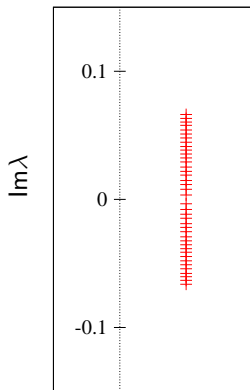
$$\lim_{m \rightarrow 0} \frac{2m}{\lambda_n^2 + m^2} \longrightarrow \pi\delta(0)$$

Chiral condensate \implies Density of Near-Zero modes.

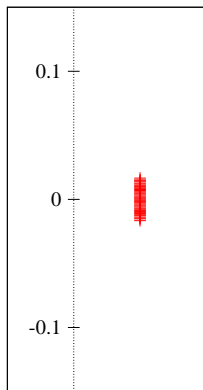
$$\bar{\psi}\psi = \frac{\pi\rho(0)}{V}$$

\rightarrow Banks, Casher, 1980

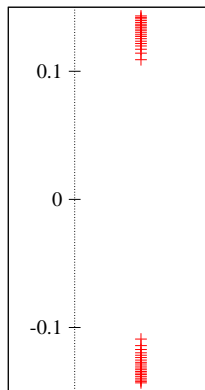
original (full)



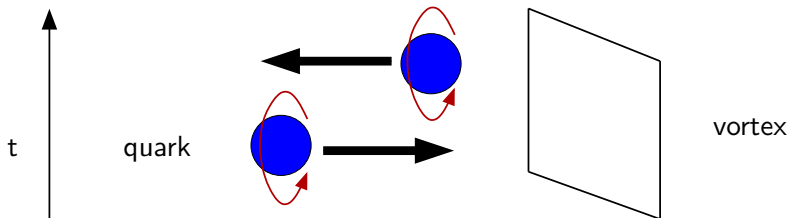
vortex only



vortex removed



QCD Dynamics break Chiral Symmetry



Strong indications that Center Vortices explain
Confinement and Chiral Symmetry Breaking.

Energy Level Displacements of Kaonic Deuterium in the Excited $2p$ State and Low-Energy $\bar{K}N$ and K^-d Scattering

M. Faber, A.N. Ivanov, M. Pitschmann
in cooperation with E.L. Kryshen and N. Troitskaya

Atominstytut der Österreichischen Universitäten,
Technische Universität Wien

March 13, 2009 / Vienna

Energy Level Displacement of Kaonic Hydrogen in the Ground State by Strong $\bar{K}N$ Low-Energy Interactions

- M. Iwasaki *et al.* (the KEK Collaboration), Phys. Rev. Lett. **78**, 3067 (1997); T. M. Ito *et al.* (the KEK Collaboration), Phys. Rev. C **58**, 2366 (1998)

$$-\epsilon_{1s}^{(\text{exp})} + i \frac{\Gamma_{1s}^{(\text{exp})}}{2} = (-323 \pm 63 \pm 11) + i(204 \pm 108 \pm 50) \text{ eV}$$

- G. Beer *et al.* (the DEAR Collaboration), Phys. Rev. Lett. **94**, 212302 (2005)

$$-\epsilon_{1s}^{(\text{exp})} + i \frac{\Gamma_{1s}^{(\text{exp})}}{2} = (-193 \pm 37 \pm 6) + i(125 \pm 56 \pm 15) \text{ eV}$$

Deser-Goldberger-Baumann-Thirring-Trueman formula

$$-\epsilon_{1s} + i \frac{\Gamma_{1s}}{2} = \frac{2\pi}{\mu} \tilde{a}_{K^-p} |\Psi_{1s}(0)|^2 = 2 \alpha^3 \mu^2 \tilde{a}_{K^-p}$$

$$f(k)_{K^-p} = \frac{1}{2ik} \left(\eta(k) e^{i2\delta(k)} - 1 \right) \Big|_{k=0} = \tilde{a}_{K^-p} = \text{Re } \tilde{a}_{K^-p} + i \text{Im } \tilde{a}_{K^-p}$$

Experimental data

$$\tilde{a}_{K^-p}^{\text{KEK}} = (-0.784 \pm 0.153 \pm 0.027) + i(0.494 \pm 0.252 \pm 0.121) \text{ fm}$$

$$\tilde{a}_{K^-p}^{\text{DEAR}} = (-0.468 \pm 0.090 \pm 0.015) + i(0.302 \pm 0.135 \pm 0.036) \text{ fm}$$

Measurement of Energy Level Displacements

Analysis of X-ray from $(K^-p)_{2p} \rightarrow (K^-p)_{1s} + \gamma$ transitions

$$n \simeq \sqrt{\frac{\mu_K}{m_e}} = 25 \quad \mu_K = \frac{m_K m_p}{m_K + m_p} = 323.5 \text{ MeV}$$

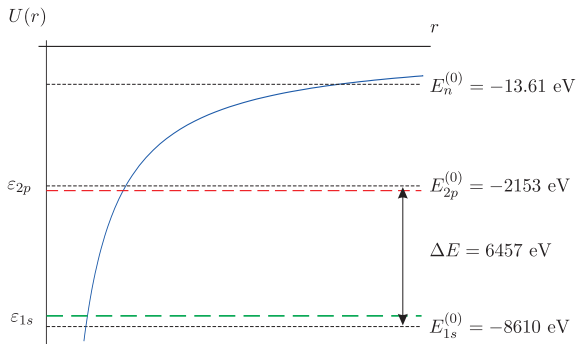
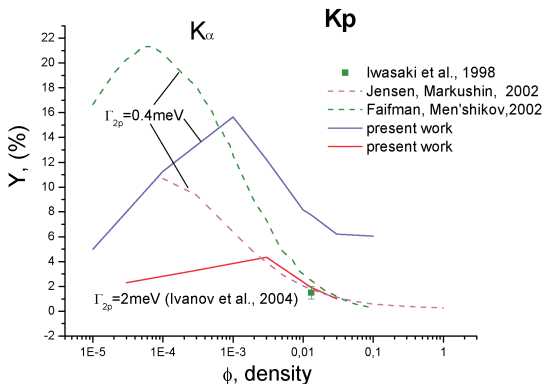
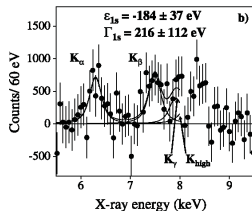
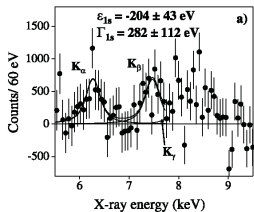


Figure: Cascade transitions of kaonic hydrogen $(K^-p)_n \rightarrow (K^-p)_{2p}$.

Experimental X-Ray Spectra

Mark Faifman (EXA2005) : $Y^{\text{exp}} = (1.1 \pm 0.3) \%$



T. Koike *et al.*, Phys. Rev. C **53**, 79 (1996): $\Gamma_{2p} > 1 \text{ meV}$

A.N.I. *et al.*, Phys. Rev. A **71**, 052508 (2005): $\Gamma_{2p} = 2 \text{ meV}$

S-wave Scattering Length of Kaonic Deuterium

$$-\epsilon_{1s} + i\frac{\Gamma_{1s}}{2} = 2\alpha^3 \mu^2 \tilde{a}_{K-d}$$

$$\rightarrow \tilde{a}_{K-d} = \frac{m_d}{m_K + m_d} \int d^3x |\Phi_d(\vec{r})|^2 \hat{A}_{K-d}(r)$$

Faddeev equation: $T_{K-d} = T_p + T_n$

S. S. Kamalov *et al.*, Nucl. Phys. A **690**, 494 (2001)

$$T_p = t_p + t_p G_0 T_n + t_p^x G_0 T_n^x$$

$$T_n = t_n + t_n G_0 T_p$$

$$T_n^x = t_n^x + t_n^0 G_0 T_n^x + t_n^x G_0 T_n$$

Faddeev Equation in the Diagram Representation: S. S. Kamalov *et al.*, Nucl. Phys. A **690**, 494 (2001)

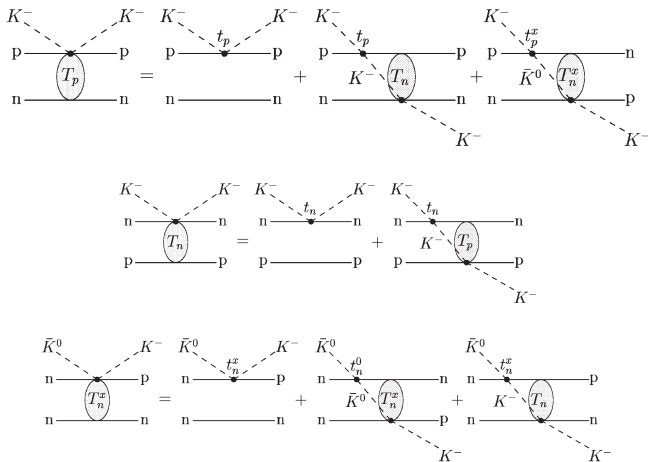


Figure: The Faddeev equation for the S-wave amplitude of low-energy $K^- d$ scattering in the diagram representation

Fixed centre approximation (FCA)

$$\hat{A}_{K-d}(r) = \frac{\hat{a}_p + \hat{a}_n + \frac{2\hat{a}_p\hat{a}_n}{r} - \frac{\hat{a}_x^2}{r + \hat{a}_n^0} - \frac{2\hat{a}_x^2\hat{a}_n}{r(r + \hat{a}_n^0)}}{1 - \frac{\hat{a}_p\hat{a}_n}{r^2} + \frac{\hat{a}_x^2\hat{a}_n}{r^2(r + \hat{a}_n^0)}}.$$

$$\hat{a}_p = \left(1 + \frac{m_K}{m_N}\right) \tilde{a}_{K-p}(K^-p) \quad , \quad \hat{a}_n = \left(1 + \frac{m_K}{m_N}\right) \tilde{a}_{K-n}(K^-n),$$

$$\hat{a}_x = \left(1 + \frac{m_K}{m_N}\right) \tilde{a}_{K-p}(\bar{K}^0n) \quad , \quad \hat{a}_n^0 = \left(1 + \frac{m_K}{m_N}\right) \tilde{a}_{\bar{K}^0n}(\bar{K}^0n),$$

P-wave Scattering Length of Kaonic Deuterium

Energy level displacement of kaonic deuterium in $2p$ state

$$\epsilon_{np} = -\frac{2}{3} \frac{\alpha^5}{n^3} \left(1 - \frac{1}{n^2}\right) \left(\frac{m_K m_d}{m_K + m_d}\right)^4 \operatorname{Re} \tilde{a}_{K^-d}^{(1)}(K^-d),$$

$$\Gamma_{np} = \frac{4}{9} \frac{\alpha^5}{n^3} \left(1 - \frac{1}{n^2}\right) \left(\frac{m_K m_d}{m_K + m_d}\right)^4 \operatorname{Im} \tilde{a}_{K^-d}^{(1)}(K^-d)$$

Faddeev equation

$$T_p^{(1)} = t_p^{(1)} + t_p^{(1)} G_0 T_n^{(0)} + t_p^{(0)} G_0 T_n^{(1)} + t_p^{x(1)} G_0 T_n^{x(0)} + t_p^{x(0)} G_0 T_n^{x(1)},$$

$$T_n^{(1)} = t_n^{(1)} + t_n^{(1)} G_0 T_p^{(0)} + t_n^{(0)} G_0 T_p^{(1)},$$

$$T_n^{x(1)} = t_n^{x(1)} + t_n^{0(1)} G_0 T_n^{x(0)} + t_n^{0(0)} G_0 T_n^{x(1)} + t_n^{x(1)} G_0 T_n^{(0)} + t_n^{x(0)} G_0 T_n^{(1)}.$$

Solution of the Faddeev equation in the FCA

$$\tilde{a}_{K^-d}^{(1)} = \frac{m_d}{m_K + m_d} \int d^3x |\Phi_d(\vec{r})|^2 \hat{A}_{K^-d}^{(1)}(r)$$

$$\hat{A}_{K^-d}^{(1)}(r) = \hat{A}_p^{(1)}(r) + \hat{A}_n^{(1)}(r)$$

Solution of the Faddeev equation in the FCA

$$\hat{A}_{K-d}^{(1)}(r) = \hat{A}_p^{(1)}(r) + \hat{A}_n^{(1)}(r)$$

$$\hat{A}_p^{(1)}(r) = \frac{F_p(r) + \left[\frac{2}{3} \frac{a_p^{(0)}}{r} - \frac{\frac{4}{9} \left(\frac{a_x^{(0)}}{r} \right)^2}{1 + \frac{2}{3} \frac{a_n^{(0)}}{r}} \right] F_n}{1 - \frac{4}{9} \frac{a_p^{(0)} a_n^{(0)}}{r^2} - \frac{\frac{8}{27} \left(\frac{a_x^{(0)}}{r} \right)^2 \frac{a_n^{(0)}}{r}}{1 + \frac{2}{3} \frac{a_n^{(0)}}{r}}}$$

$$\hat{A}_n^{(1)}(r) = F_n(r) + \frac{2}{3} \frac{\hat{a}_n^{(0)}}{r} \hat{A}_p^{(1)}(r)$$

$$F_p(r) = a_p^{(1)} + \frac{2}{3} \frac{a_p^{(1)}}{r} \hat{A}_n^{(0)}(r) - \frac{2}{3} \frac{a_x^{(1)}}{r} \hat{A}_n^{x(0)}(r)$$

$$F_n(r) = a_n^{(1)} + \frac{2}{3} \frac{a_n^{(1)}}{r} \hat{A}_p^{(0)}(r)$$

Theoretical Basis of our Researches

Chiral Lagrangians with $SU(3) \times SU(3)$ chiral symmetry

$$\begin{aligned}\mathcal{L}_{\text{int}}[P(x), B(x), B(x), \dots] &= \\ &= \langle \bar{B}(x) i \gamma^\mu [s_\mu(x), B(x)] \rangle \\ &- g_A (1 - \alpha_D) \langle \bar{B}_j(x) \gamma^\mu [p_\mu(x), B(x)] \rangle - g_A \alpha_D \langle \bar{B}(x) \gamma^\mu \{p_\mu(x), B(x)\} \rangle \\ &+ g_{\Lambda^*} \bar{\Lambda}^*(x) \gamma^\mu \gamma^5 \langle p_\mu(x) B(x) \rangle \\ &+ \langle \bar{B}_j(x) i \gamma^\mu [s_\mu(x), B(x)] \rangle \\ &- g_{A_j} (1 - \alpha_{D_j}) \langle \bar{B}_j(x) \gamma^\mu [p_\mu(x), B(x)] \rangle - g_{A_j} \alpha_{D_j} \langle \bar{B}_j(x) \gamma^\mu \{p_\mu(x), B(x)\} \rangle \\ &\sqrt{2} g_A \bar{D}_\mu^{abc}(x) \Theta^{\mu\nu} \gamma^5 (p_\nu(x))_a^d B_b^e(x) \varepsilon_{cde}\end{aligned}$$

$$B(\underline{\mathbf{8}}) = (p, n, \Lambda^0, \Sigma, \Xi), \Lambda^* = \Lambda^0(1405)(\underline{\mathbf{1}})$$

$$B_1(\underline{\mathbf{8}}) = (N(1440), \Lambda(1600), \Sigma(1660))$$

$$B_2(\underline{\mathbf{8}}) = (N(1710), \Lambda(1810), \Sigma(1880))$$

$$D(\underline{\mathbf{10}}) = (\Delta(1232), \Sigma^*(1385), \dots)$$

Experimental ratios of cross sections for inelastic K^-p scattering at threshold

$$\gamma = \frac{\sigma(K^-p \rightarrow \Sigma^- \pi^+)}{\sigma(K^-p \rightarrow \Sigma^+ \pi^-)} = 2.360 \pm 0.040$$

$$R_c = \frac{\sigma(K^-p \rightarrow \Sigma^- \pi^+) + \sigma(K^-p \rightarrow \Sigma^+ \pi^-)}{\sum_{Y\pi} \sigma(K^-p \rightarrow Y\pi)} = 0.664 \pm 0.011$$

$$R_n = \frac{\sigma(K^-p \rightarrow \Lambda^0 \pi^0)}{\sigma(K^-p \rightarrow \Sigma^0 \pi^0) + \sigma(K^-p \rightarrow \Lambda^0 \pi^0)} = 0.189 \pm 0.015.$$

Experimental data on S-wave K^-p scattering length by SMI

$$\tilde{a}_{K^-p}^{DEAR} = (-0.468 \pm 0.090 \pm 0.015) + i(0.302 \pm 0.135 \pm 0.036) \text{ fm}$$